JOURNAL OF MATERIALS SCIENCE 17 (1982) 2585–2593

Thermoluminescent mechanisms involving transition metal ion impurities and V-type centres in MgO crystals exposed to ultraviolet radiation

W. C. LAS,* T. G. STOEBE
Department of Mining, Metallurgical and Ceramic Engineering, University of Washington, Seattle, WA 98195, USA

Thermoluminescent (TL) mechanisms involving Fe, Cr, Mn and V ions in both divalent and trivalent valence states, and V-type centres were studied in MgO single crystals of varying impurity content after exposure to ultraviolet radiation. Using the ESR technique, it is shown that samples containing primarily divalent impurities show no V-type centres related to the TL mechanism, which is that of charge transfer between the impurities. V-type centres, when present, are seen to be more stable in purer samples than in less pure samples, resulting in a shift of the TL peaks to higher temperatures. The TL mechanism in this case includes charge transfer between V-type centres and the impurities. The supralinear behaviour of TL peak 1 is associated with the R-emission lines of Cr^{3+}.

1. Introduction

The optical and magnetic properties of MgO, as influenced by ionizing radiations such as X-rays [1–3] and γ-rays [4–6], and by ultraviolet (u.v.) light [1, 7–11], have been studied extensively. Changes in impurity-related properties have been also investigated using various heat treatments [3, 12–14] and valence changes directed using electron spin resonance (ESR) [3, 12, 15] and optical absorption (OA) [12, 16] techniques. These studies have indicated that charge transfer between V-type centres and impurities such as Fe, Cr, Mn and V in particular valence states play an important role in the mechanism for thermoluminescence (TL) in this material. The current understanding of the role of these impurities in the TL or MgO is not yet completely established, however, particularly in relation to the effects of u.v. irradiation in this material.

2. Background

The most common defects encountered in MgO are V-type centres. The simplest of these consists of one hole trapped at the Mg^{2+} ion vacancy with the hole being shared by the next-neighbour oxygen. Sonder and Sibley [17] refer to this as the V^- centre. When association with a trivalent impurity, usually a transition metal ion M, it is denoted V_M. The optical and magnetic properties and thermal stabilities of a large number of these centres have been well documented [18–22]. Henderson *et al.* [23], using ESR, report an axially symmetric spectrum of Fe^{3+} in MgO, denoted as the Fe^{3+} [100] centre, arising from the presence of next-nearest-neighbour vacancies along the [100] direction. Krishnan [11] studied MgO crystals exposed to u.v. radiation using the ESR technique and identified Fe^{3+} ions in both distorted octahedral and tetragonal sites. The observed emissions at 654 nm and 659 nm were attributed to these two defects, respectively, and calculations of possible transitions based on the Tanabe–Sugano diagram for Fe^{3+} agreed with these two emission lines [11]. Wertz and Auzins [24] report ESR lines for Cr^{3+} ions in tetragonal and rhombic symmetries in addition to the Cr^{3+} ions in cubic sites. These dif-

* Present address: Instituto de Pesquisas Energeticas e Nucleares, CP 11049, Pinheiros, San Paulo, SP, Brasil.

0022–2461/82/092585–09$03.58/0

ferent field symmetries associated with ions such as Fe^{3+} and Cr^{3+} could play an important role in charge transfer mechanisms. Infrared absorption measurements have been helpful in identifying centres due to the OH-bond stretching vibration, such as the V_{OH}^- and V_{OH} centres [18, 25, 26] which can also be associated with trivalent impurities [25–27].

Although it has been observed that Fe^{3+}, Cr^{3+} and V^{2+} may change valence depending on the treatment, it has been generally accepted that the valence state and concentration of Mn^{2+} does not change upon heat treatment, X-irradiation or u.v. excitation [3, 11, 15, 28], nor does it change after passage of an electric current at high temperature [29]. However, Challis *et al.* [30] concluded indirectly that 1 to 2% of the Mn in Mn-doped MgO is present as Mn^{3+}, and Sibley *et al.* [31] have observed changes in Mn^{2+} concentration in deformed and γ-irradiated MgO. We have also shown that under certain circumstances, the valence state of Mn does change [32].

The TL emission in MgO has been reported as partially the result of holes captured by Fe^{2+} ions, giving rise to the $Fe^{3+*} \rightarrow Fe^{3+}$ transition [11, 31]. There is disagreement, however, as to the energy of the TL emission: X-, γ- or electron-excited crystals usually emit in the blue and red regions [31, 33–35] while u.v.-irradiated crystals show only an orange component [10, 11]. Our observations indicate that u.v. radiation, as compared to radiations of higher energy, is not energetically efficient enough to cause the blue luminescence, although both blue and orange emissions can be the result of transitions from different excited states of Fe^{3+} to the corresponding ground state. The only well-established TL emission lines in MgO are the R-lines ascribed to the $Cr^{3+*} \rightarrow Cr^{3+}$ transition and corresponding to TL peak 1 [1].

3. Experimental procedure

MgO single crystals were supplied by Norton Co. and by W. C. Spicer, the former having a higher total impurity concentration than the latter, as shown in Table I. Relative impurity concentrations were measured by ESR, using a Varian spectrometer model V-4502 operating in the X-band at room temperature. The crystals were exposed to non-monochromatic filtered u.v. light from an Hg source and/or to monochromatic light in the region 250–360 nm. The optical system consisted of a 200 W Hg lamp in a Schoeffel lamp-housing and power supply, a Jarrell-Ash 82410, 0.25 Metre Ebert monochromator and an EG & G radiometer with a detector head model 580-20A; the total irradiance, I_t, is reported in W sec cm^{-2}. A Corning filter, type 7-54, transmitting about 86% at 320 nm and 5% at 240 nm and 410 nm, was used in all experiments. Heat treatments were performed in air at 1000° C and 1400° C for periods ranging from 3 to 24 h, all samples being quenched to room temperature within a period of 5 min. The TL was recorded in a Harshaw TL reader model 2000, with a heating rate of 1° C sec^{-1}; the TL output is reported in $A g^{-1}$; the maximum temperature of a TL reading is represented by T_m, usually 250° C unless otherwise indicated. Infrared absorption measurements were performed in a Perkin–Elmer spectrometer model 727B, in the region 4000–600 cm^{-1}, with a resolution of 3 cm^{-1}.

The TL of a material is characterized by the emission of light which results when the energy stored by radiation is released by thermal excitation. The emitted light recorded as a function of temperature constitutes the TL glow curve. Relative impurity concentrations were measured before and after the u.v. exposure and after the TL reading. The concentration ratios before u.v. to after u.v., and after u.v. to after TL, denoted respectively as R_1 and R_2, indicate changes in the valence state of the impurity ion considered. These ratios together with the characteristics of the TL glow curves of each material are utilized in the analysis of the processes involved in the u.v. exposure and the TL phenomenon. Fading of the TL signal was measured as the loss of sensitivity of each TL peak after exposing the samples to u.v. light and keeping them in the dark at room temperatures for different intervals of time. The investigation of fading indirectly gives information about the type of trapping centres in MgO. Partial TL readings consisted of studying separately each TL peak and measuring the corresponding R_1 and R_2 ratios, in order to investigate the mechanisms for each TL peak rather than for the overall glow curve.

4. Results and discussion

4.1. Glow curve structure

Typical TL glow curves for MgO exposed to non-monochromatic u.v. radiation are shown in Fig. 1 for Norton and Spicer crystals. The major differences between these materials are the overall TL sensitivity, the temperature of the TL peaks

TABLE I Concentrations of Fe, Cr, Mn and V in Norton and Spicer samples. Total concentrations from spectrographic analysis (t), ion concentration from ESR, and ESR peak-to-peak line width are shown for each

Sample	Fe_t (ppm)	Fe^{3+} (ppm)	ΔH_{pp} (G)	Cr_t (ppm)	Cr^{3+} (ppm)	ΔH_{pp} (G)	Mn_t (ppm)	Mn^{2+} (ppm)	ΔH_{pp} (G)	V_t (ppm)	V^{2+} (ppm)	ΔH_{pp} (G)
Norton:												
I (NP3)	110	18	4.75	< 10	7	1.04	9	5	1.16	–	–	–
(NP0)	150	34	4.75	–	5	1.13	11	5	1.32	–	–	–
II	400	1.5	5.09	20	0.3	1.05	< 10	6	1.19	–	8	0.6
III	470	16	5.72	–	2	0.97	20	7	1.07	–	–	–
Spicer	< 50	2	4.35	< 10	0.5	0.98	0.7	0.3	1.02	0.6	0.2	0.55

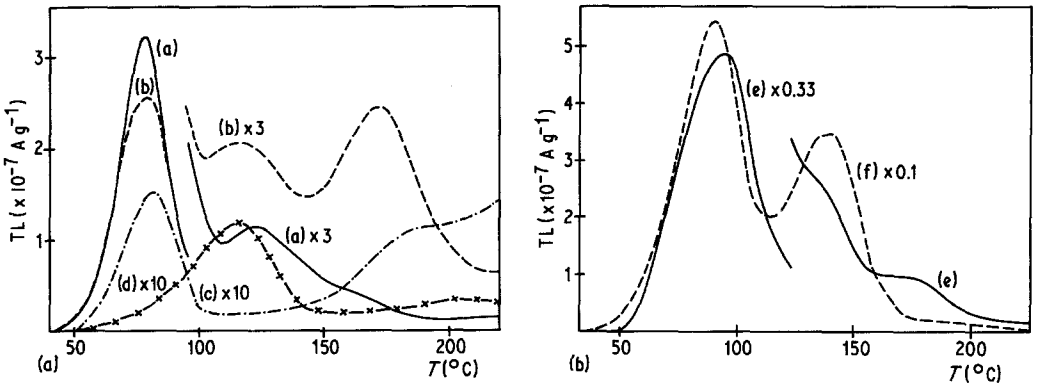

Figure 1 TL glow curves for MgO exposed to non-monochromatic u.v. radiation, 27.6 W sec cm^{-2}. (a) Norton sample, Group I, "as-received"; (b) Norton sample, Group I, heat treated in air at 1400° C for 24 h; (c) Norton sample, Group II, "as-received"; (d) Norton sample, Group III, "as-received"; (d) Spicer sample, "as-received"; and (f) Spicer sample, heat treated in air at 1400° C for 3 h.

and the sensitization behaviour after annealing in air. Norton samples were classified into three groups, I, II and III, according to the dominant peak temperature and the TL mechanisms, as discussed below. Spicer crystals have a higher TL sensitivity than Norton crystals, probably as a consequence of the concentration quenching effect, since Spicer samples are purer than Norton ones; this is also seen in Norton samples, where Group I has a lower impurity content and, therefore, a higher sensitivity than Groups II and III, as shown in Fig. 1. The glow curves are composed of a variable number of TL peaks, depending on the crystal group and treatments. There are at least three peaks, which we number 1 to 3, the lower-temperature peak being dominant. The TL peaks in Spicer crystals are shifted to higher temperatures by approximately 20° C, as compared to corresponding peaks in Norton samples from Group I. Annealing Norton samples in air at 1400° C causes the sensitization of TL Peak 3 and, to a smaller extent, of TL Peak 2, as shown in Fig. 1, Curve b. TL Peak 1 is not sensitized and, in some cases, it even decreases slightly after the heat treatment. After a 1400° C annealing, Spicer samples are sensitized in a different way: the effect occurs mainly for TL Peak 2, somewhat for TL Peak 1, but not at all for TL Peak 3, as shown in Fig. 1, Curve f.

4.2. Fading

Fading of the TL signal was investigated with the objective of comparing the behaviour of Spicer and Norton crystals, Group I, as shown in Fig. 2. One notes that Curves a, b and c are not single exponentials. By comparing Curves a and c, it is evident that the 96° C TL Peak 1 in Spicer crystal is much more stable than the 76° C TL Peak 1 in Norton crystal. It is known that centres such as V_{Al} and V_{OH} have a half-life of the order of a few hours [19]; this could be responsible for the rapid fading behaviour of the 76° C TL Peak 1 in the MgO Norton samples, Group I. However, our samples showed no V_{OH} centres, only V^-_{OH} and these do not take part in the TL mechanisms, according to the infrared results presented below. In addition, it will be seen that a 1400° C treatment annealed out the V^-_{OH} centres present in the "as received" samples, but there was no difference in fading behaviour between annealed and non-

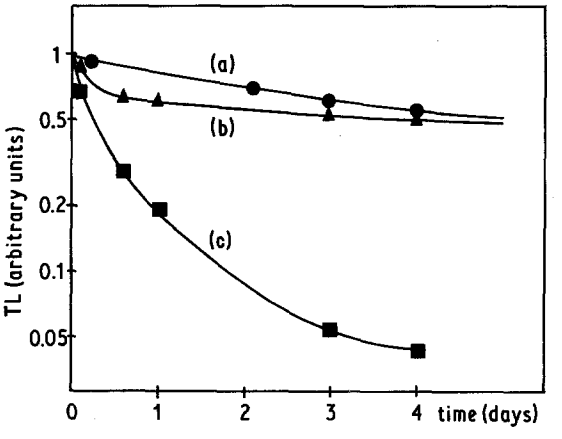

Figure 2 TL fading characteristics for MgO samples. (a) Spicer, "as-received", 96° C TL peak 1, non-monochromatic u.v. radiation, 27.6 W sec cm^{-2} (•); (b) Norton Group I, "as-received", 125° C TL peak 2, 289 nm, 0.2 W sec^{-1} (▲); and (c) Norton Group I, "as-received", 76° C TL peak 1, 289 nm, 0.2 W sec^{-2} (■).

annealed samples. If the V_{Al} centres have a room-temperature stability which is not represented by a single exponential, then these centres could be the traps of the 76° C TL Peak 1. If the stability of the V_{Al} centre follows a single exponential, then other V-type centres in addition to V_{Al} are required to explain this fading behaviour.

The same reasoning would apply to higher temperature peaks, where impurity-related V-centres, with higher stabilities than those responsible for TL Peak 1 in Norton samples, would account for this slower fading. This is seen in Fig. 2, Curve b, where the 125° C TL Peak 2 in Norton samples shows a slower fading than the 76° C TL Peak 1. TL Peaks 2 and 3, when present, were observed to decay slower than TL Peak 1 in both Norton and Spicer crystals. In trying to assign the trapping centres for the 125° C TL Peak 2 in Norton and the 96° C TL Peak 1 in Spicer samples, some inconsistencies appear, since the former is at a higher temperature than the latter, and fading indicates that the 125° C TL peak is less stable than the 96° C TL peak. It seems, therefore, that trapping centres responsible for these peaks cannot be compared on the basis of thermal stability and peak temperatures alone.

It is known [22] that at room temperature, the ESR signal at $g_\perp = 2.0385$ is due to V_{Al} or V_M centres, while the V^- centre is isotropic, with $g_{iso} = 2.0267$. The fading of the V_M line was investigated in both crystals. In Norton samples, Group I, this signal decayed about 75% after storage for 70 h following u.v. exposure, while in Spicer samples, the decay was 25% for the same period of time. One particular Spicer crystal left in the dark for four months showed a decrease in TL Peak 1 amplitude of only a factor of 12. These results indicate that most of the trapping centres in Spicer samples are probably a highly stable variety of V_M centres. V_{Al} centres, if present at all in Spicer samples, must account for a very small fraction of the trapping centres. Indeed, one would expect more impurity-associated V-type centres in Norton samples, since they contain a larger number of impurities. However, Norton samples from Groups II and III showed no ESR signal from V_M centres, possibly because most of the Fe ions are in the divalent state, as seen in Table I, thus requiring only a few vacancies for charge compensation. On the other hand, these latter samples contain Cr^{3+} [100] in a larger concentration than samples of Group I; these centres were not further investigated as far as the TL mechanisms are concerned.

Although there is no direct evidence, the V_M centres responsible for part of the fading characteristics would probably include V^- centres in association with Fe ions. The Fe^{3+} [100] centre observed by Henderson *et al.* [23] would be the precursor of the V_{Fe} ($M = Fe$) centre, which is formed upon u.v. irradiation in such a way that a hole released from the Fe^{3+} ion is captured at the oxygen ion opposite the vacancy. This configuration can be rather unstable, for the hole would tend to reassociate with the Fe^{2+} ion, thus explaining the fading behaviour at room temperature.

The stability of the V_{Fe} centre is assumed to be between that of the V_{Al} and V^- centres, corresponding to the initial decay of Curves a and b in Fig. 2. Since these are not coincident, it could be that different Fe^{3+}-associated vacancies, in addition to those in the tetragonal Fe^{3+} [100] centre, are involved. One piece of evidence for this is in Table I, where the ESR linewidth is seen to vary among the different samples: the linewidth is smaller in the purer crystals, where the interaction between vacancies and a few impurities is believed to lead to more stable trapping centres and thus to higher activation energies for the TL peaks. For this reason, the TL peaks in Spicer samples are shifted to higher temperatures relative to the TL peaks in Norton samples, Group I.

The isotropic V^- line was observed for both Norton and Spicer crystals heat-treated in air at 1400° C after exposure to non-monochromatic u.v. light. This line was present even after the TL reading of Spicer samples, agreeing with the known high V^- centre stability.

4.3. Mechanisms for TL

Infrared absorption measurements show bands at 3310 cm^{-1} and 3550 cm^{-1} in Norton crystals, Group I, and at 3296 cm^{-1} and 3690 cm^{-1} in Spicer crystals. The 3296 cm^{-1} and 3310 cm^{-1} lines are due to V_{OH}^- centres [18] and V_{OH}^- associated with trivalent impurities [25, 27], respectively. The lines at 3550 cm^{-1} and 3690 cm^{-1} are probably due to precipitates [26]. The infra-red spectrum was unchanged after u.v. irradiation and TL reading. One would expect that the holes released by u.v. light would be captured at V_{OH}^- centres, forming the V_{OH} centres at 3323 cm^{-1}, but this is not observed. Since the

TABLE II Ratios of concentrations, determined using ESR. R_1, before u.v. to after u.v. exposure; R_2, after u.v. to after TL read out. Ultravoilet exposure to (a)non-monochromatic u.v. light, (b) 249 nm light, or (c) 289 nm light, as noted

Sample	Fe^{3+}		Cr^{3+}		Mn^{2+}		V^{2+}	
	R_1	R_2	R_1	R_2	R_1	R_2	R_1	R_2
Norton:								
"as-received"								
I (b)	1.15	0.80*	1.21	0.81*	1.02	0.94	–	–
(a)	1.12	0.82*	1.03	0.95	0.93	1.05	–	–
II (a)	1.75	0.85	1.02	0.97	1.23	0.96	–	–
III (a)	1.34	0.88*	0.15	2.18	1.01	0.98	–	–
air-heated-treated 1400° C/24 h.								
I (a)	1.45	0.90	0.93	1.02*	2.02	1.02	–	–
Spicer:								
"as-received"								
(a)	3.36	0.37	1.03	1.04	0.74	1.40*	0.58	1.08
(c)	1.95	0.64	1.10	0.98	0.92	1.15*	1.24	0.88*
air-heat-treated 1400° C/3 h.								
(a)	2.74	0.41	1.02	1.02	0.92	1.60	0	1.06

* Denotes a return to the original state, $R_2 = 1/R_1$.

V_{OH} band seems to appear with γ-irradiation [18], our results can be interpreted by saying that the u.v. energy is not high enough to fill the V_{OH}^- centres with holes. Therefore, these centres do not take part in the TL process. While after heat treatments at 1000° C the infrared bands were still present, they vanished after heat treatments in air and in a reducing atmosphere of CO and CO_2 at 1400° C. This means that the V_{OH}^- centres are indirectly related to the TL mechanisms, since at 1400° C in air, vacancies that dissociate from V_{OH}^- and related centres contribute to the formation of trapping centres such as V^- and V_M.

Table II summarizes the ratios of impurity concentrations, R_1 and R_2, for both materials. Ratios between 0.90 and 1.10 are not considered to be real changes when allowance for the uncertainty in the ESR results is made; a return to the original state is denoted with a star if R_2 is the inverse of R_1. The changes in Fe^{3+} concentration are seen to be larger in Spicer than in Norton crystals. Changes in Mn^{2+} concentration in Norton samples occur in a few cases, and seem to be opposite to those of Spicer crystals; in Norton samples, the Mn^{2+} content does not return to its original value after the TL reading, since R_2 is approximately 1.0. The Cr^{3+} content changes only in Norton, Group III, and for the exposure of 294 nm in Group I; it also decreases in "as received" Spicer crystals exposed to 249 nm, this result not being shown in the table. The behaviour of V^{2+}, which is observed only in Spicer samples, differs depending on the u.v. treatment, as indicated in Table II. The influence of V^{2+} on the TL mechanisms is reported elsewhere [37].

Based on the results above, TL mechanisms may be proposed, as indicated by the equilibrium reactions given in Table III. These include charge transfer processes between impurity ions and V-type centres for Spicer samples and Norton crystals, Group I, and a direct charge transfer mechanism between impurity ions, without involving V-type centres, for Norton crystals, Groups II and III. The major centres activated by non-monochromatic light are identified as Fe^{3+} in Norton samples and Fe^{3+}, Mn^{3+} and V^{3+} in Spicer crystals. As suggested by the stability characteristics, the principal trapping centres filled with holes by u.v. radiation could be V_{Al} and V_M centres in Norton, Group I, and V_M and V^- centres in Spicer samples.

The recombination centre common to all samples and, as seen later, to all TL peaks, is the Fe^{2+} ion. As was seen in Table II, Spicer crystals are more efficient as to the $Fe^{3+} \xrightarrow{u.v.} Fe^{2+} \xrightarrow{TL} Fe^{3+}$ conversion than Norton crystals and, accordingly, the overall TL sensitivity is higher for Spicer samples.

Mn^{2+} is also a recombination centre in Spicer, but not in Norton samples. In Norton samples, this ion is identified rather as a hole trap, since its con-

TABLE III Equilibrium reactions caused by u.v. irradiation and TL read out. Ultraviolet treatments (a), (b), (c), as in Table II. V^{2-} represents a non-ionized vacancy; V^{-} represents a vacancy with one trapped hole; V_{Al} and V_M represent a vacancy near an Al or other metal cation M, with one trapped hole.

Norton "as-received"

Group I

$$[Fe^{3+}] + [Cr^{3+}] + V^{2-} \underset{TL}{\overset{(b)}{\rightleftharpoons}} [Fe^{2+}] + [Cr^{2+}] + V_{Al} + V_M$$

$$[Fe^{3+}] + V^{2-} \underset{TL}{\overset{(a)}{\rightleftharpoons}} [Fe^{2+}] + V_{Al} + V_M$$

Group II

$$[Fe^{3+}] + [Mn^{2+}] \xrightarrow{(a)} [Fe^{2+}] + [Mn^{3+}]$$

$$[Fe^{2+}] \xrightarrow{TL} [Fe^{3+}]$$

Group III

$$[Fe^{3+}] + [Cr^{2+}] \underset{TL}{\overset{(a)}{\rightleftharpoons}} [Fe^{2+}] + [Cr^{3+}]$$

Norton air-heat-treated:

Group I

$$[Fe^{3+}] + [Mn^{2+}] + V^{2-} \xrightarrow{(a)} [Fe^{2+}] + [Mn^{3+}] + V_{Al} + V_M$$

$$[Fe^{2+}] + V_{Al} + V_M \xrightarrow{TL} [Fe^{3+}] + V^{2-}$$

Spicer "as-received":

$$[Fe^{3+}] + [Mn^{3+}] + [V^{3+}] + V^{2-} \xrightarrow{(a),(b)} [Fe^{2+}] + [Mn^{2+}] + [V^{2+}] + V_M + V^{-}$$

$$[Fe^{2+}] + [Mn^{2+}] + V_M + V^{-} \xrightarrow{TL} [Fe^{3+}] + [Mn^{3+}] + V^{2-}$$

$$[Fe^{3+}] + [V^{2+}] + [Mn^{3+}] + V^{2-} \underset{TL}{\overset{(c)}{\rightleftharpoons}} [Fe^{2+}] + [V^{3+}] + [Mn^{2+}] + V_M + V^{-}$$

Spicer air-heat-treated:

$$[Fe^{3+}] + [Mn^{3+}] + [V^{3+}] + V^{2-} \xrightarrow{(a)} [Fe^{2+}] + [Mn^{2+}] + [V^{2+}] + V_M + V^{-}$$

$$[Fe^{2+}] + [Mn^{2+}] + V_M + V^{-} \xrightarrow{TL} [Fe^{3+}] + [Mn^{3+}] + V^{2-}$$

centration decreases with u.v. light, as indicated by the equilibrium reactions of the air-heat-treated Group I and "as received" Group II Norton samples. The Mn^{2+} hole trap is tentatively ascribed to TL Peak 3, which was sensitized in Group I, as shown in Fig. 1b, and is prominent in Group II.

The trapping centres for TL Peak 2 in Norton samples, Group I, can be identified with V_{Fe} centres, since this peak was sensitized by annealing in air, which is believed to increase the V_{Fe} concentration. The dominant TL peak in samples of Group III, occurring at approximately the same temperature as TL Peak 2 in Group I, seems to be related to Cr^{2+} ions, which act as trapping centres for holes. V_{Fe} centres would also be less probable in Group II, where a TL peak at the corresponding temperature is absent, because both Groups II and III have very small concentrations of Fe^{3+} (Table I) and, therefore, very few compensations vacancies. As a matter of fact, V_M centres were not detected by ESR in these two groups. Again, the fact that TL peaks at approximately the same temperature seem to be correlated to different trapping centres shows that this type of analysis is not sufficient to identify these centres unless other techniques such as TL emission spectrum measurements are employed.

TABLE IV Concentration ratios as measured using ESR after heating to reveal TL individually from peaks 1, 2 and 3, respectively.

Spicer samples	Ions	TL_1 (T_a = 115° C)	TL_2 (T_b = 165° C)	TL_3 (T_c = 250° C)
"As-received"	Fe^{3+}	0.62	0.74	0.81
	Mn^{2+}	1.13	1.14	0.96
Air-heat-treated 1400° C/3 h	Fe^{3+}	0.91	0.82	0.75
	Mn^{2+}	1.19	1.08	1.24

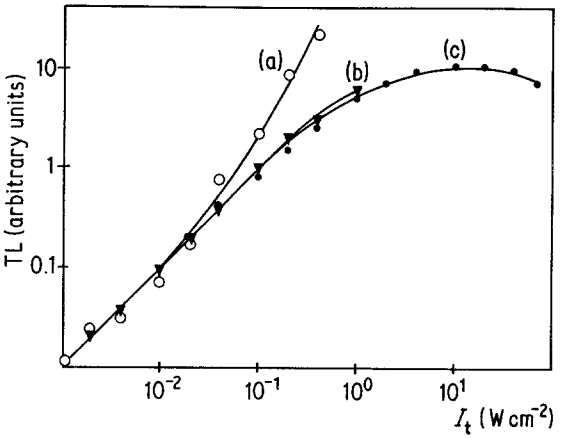

Figure 3 TL response as a function of total u.v. irradiance in "as-received" Spicer MgO exposed to (a) 249 nm (○); (b) 289 nm u.v. irradiation (▾); and (c) non-monochromatic u.v. (●).

4.4. Trapping and emission centres

In an attempt to identify the different trapping and emission centres responsible for each TL peak, a series of partial TL readings was performed consisting of the following steps:

(i) u.v. irradiation;

(ii) TL reading up to T_a, $T_1 < T_a < T_2$, to erase only Peak 1;

(iii) TL reading up to T_b, $T_2 < T_b < T_3$, to erase only Peak 2; and

(iv) TL reading up to T_c, $T_c < T_3$, to erase Peak 3.

The concentration ratios between each step are indicated for Fe^{3+} and Mn^{2+} ions in Table IV; Cr^{3+} and V^{2+} do not change during the partial TL readings. In the "as received" Spicer samples the recombination due to holes captured at Fe^{2+} and Mn^{2+} ions is more efficient at low temperatures, accounting for the high sensitivity of TL Peak 1. In air-heat-treated samples the same ions were involved, but the behaviour is reserved, that is, the recombination increases its efficiency with temperature. This sensitization effect occurs for Peaks 1 and 2, but not for Peak 3, possibly due to thermal quenching of the luminescence efficiency. The results indicate, therefore, that the transition $Mn^{3+*} \rightarrow Mn^{3+} + h\nu$ accounts for some part of the TL emission and that also the transition $Fe^{3+*} \rightarrow Fe^{3+} + h\nu$ is partially responsible for the TL emission of all three TL peaks (where h is Planck's constant and ν is the frequency).

Fig. 3 shows the TL response as a function of the total irradiance, I_t, for 249 nm (Curve a); 289 nm (Curve b); and non-monochromatic light (Curve c). All curves show an initial linear TL response; but while Curves a and c saturate at about 10 W sec cm^{-2}, Curve b is supralinear above 10^{-2} W sec cm^{-2}. This behaviour is typical for both Spicer and Norton samples. TL glow curves of MgO exposed to 249 nm are shown in Fig. 4, where it can be seen that TL Peak 1 is actually composed of two peaks, the lower temperature one being the regular peak in Norton samples, and the other, in Spicer. The appearance of a second peak excited by the 249 nm radiation causes the observed supralinearity. It has been shown in Table II that the Cr^{3+} content changes for 249 nm irradiation, where the transition $Cr^{3+*} \rightarrow Cr^{3+} + h\nu$ should occur during the TL read-out. TL Peak 1 in MgO has been correlated to the Cr^{3+}-R emission lines [1], which are observed in X-irradiated samples. Our results indicate that only high u.v. energies, such as 249 nm, make this process observable in u.v.-irradiated MgO.

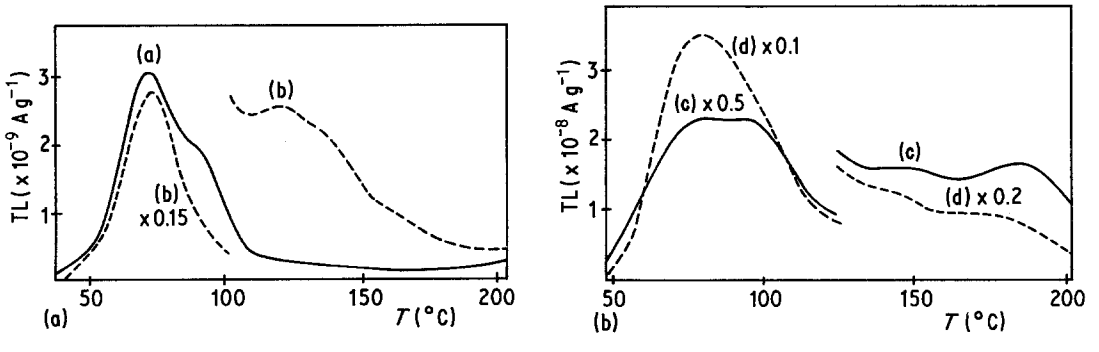

Figure 4 TL glow curves for "as-received" MgO exposed to 249 nm u.v. irradiation. (a) Norton sample, Group I, 5 × 10^{-3} W sec cm^{-2}; (b) Norton sample, Group I, 2 × 10^{-2} W sec cm^{-2}; (c) Spicer sample, 4 × 10^{-2} W sec cm^{-2}; and (d) Spicer sample, 2 × 10^{-1} W sec cm^{-2} u.v. irradiance.

References

1. J. E. WERTZ, L. C. HALL, J. HEGELSON, C. C. CHAO and W. S. DYKOSKI, in "Interaction of Radiation with Solids", Edited by A. Bishay (Plenum Press, New York, 1967) p. 617.
2. K. H. LEE and J. H. CRAWFORD, Jr, *J. Lumin.* **20** (1979) 9.
3. J. E. WERTZ, J. W. ORTON and P. AUZINS, *J. Appl. Phys. Suppl.* **33** (1962) 322.
4. Y. KIRSH, N. KRISTIANPOLLER and R. CHEN, *Phil. Mag.* **35** (1977) 653.
5. Y. CHEN and W. A. SIBLEY, *Phys. Rev.* **154** (1967) 842.
6. A. SATHYAMOORTHY and J. M. LUTHRA, *J. Mater Sci.* **13** (1978) 2637.
7. N. TAKEUCHI, K. INABE, J. YAMASHITA and S. NAKAMURA, *Health Phys.* **31** (1976) 519.
8. A. K. DHAR, L. A. DeWERD and T. G. STOEBE, *Med Phys.* **3** (1976) 415.
9. N. TAKEUCHI, K. INABE and J. YAMASHITA, *Phys. Chem.* **259** (1978) 321.
10. W. M. ZINIKER, J. K. MERROW and J. I. MUELLER, *J. Phys. Chem. Sol.* **33** (1972) 1619.
11. C. S. KRISHNAN, PhD Thesis, University of Washington (1973).
12. F. A. MODINE, E. SONDER and R. A. WEEKS, *J. Appl. Phys.* **48** (1977) 3514.
13. K. W. BLAZEY, *J. Phys. Chem. Sol.* **38** (1977) 671.
14. J. B. LACY, M. M. ABRAHAM, J. L. BOLDU, Y. CHEN, J. NARAYAN and H. T. TOHVER, *Phys. Rev. B* **18** (1978) 4136.
15. J. E. WERTZ, P. AUZINS, J. H. E. GRIFFITHS and J. W. ORTON, *Disc. Far. Soc.* **26** (1958) 66.
16. R. W. DAVIDGE, *J. Mater. Sci.* **2** (1967) 339.
17. E. SONDER and W. A. SIBLEY, in "Point Defects in Solids" Vol. 1, Edited by J. H. Crawford and L. M. Slifkin (Plenum Press, New York, 1972).
18. Y. CHEN, M. M. ABRAHAM, L. C. TEMPLETON and W. P. UNRUH, *Phys. Rev. B* **11** (1975) 881.
19. M. M. ABRAHAM, Y. CHEN and W. P. UNRUH, *ibid* **9** (1974) 1842.
20. L. A. KAPPERS, F. DRAVNIEKS and J. E. WERTZ, *Sol. Stat. Commun.* **10** (1972) 1265.
21. W. P. UNRUH, Y. CHEN and M. M. ABRAHAN, *Phys. Rev. Lett.* **30** (1973) 446.
22. L. A. KAPPERS, F. DRAVNIEKS and J. E. WERTZ, *J. Phys. C: Sol. St. Phys.* **7** (1974) 1387.
23. B. HENDERSON, J. E. WERTZ, J. P. HALL and R. D. DOWSING, *ibid.* **4** (1971) 107.
24. J. E. WERTZ and P. AUZINS, *Phys. Rev.* **106** (1957) 484.
25. A. M. GLASS and T. M. SEARLE, *J. Chem. Phys.* **46** (1967) 2092.
26. B. HENDERSON and W. A. SIBLEY, *ibid* **55** (1971) 1276.
27. E. R. VANCE and W. C. MALLARD, *Phys. Stat. Sol. (b)* **91** (1979) K155.
28. R. L. HANSLER and W. G. SEGELKEN, *J. Phys. Chem. Sol.* **13** (1960) 124.
29. R. A. WEEKS, E. SONDER, J. C. PIGG and K. F. KELTON, *J. Phys. (France)* **37** (1976) C7-411.
30. L. J. CHALLIS, A. A. GHAZI and K. J. MAXWELL, *J. Phys. C: Sol. St. Phys.* **12** (1979) 303.
31. W. A. SIBLEY, J. L. KOLOPUS and W. C. MALLARD, *Phys. Stat. Sol.* **31** (1969) 223.
32. W. C. LAS, R. J. MATTHEWS and T. G. STOEBE, *Nucl. Inst. Methods* **175** (1980) 1.
33. R. T. WILLIAMS, J. W. WILLIAMS, T. J. TURNER and K. H. LEE, *Phys. Rev. B* **20** (1979) 1687.
34. S. DATTA, I. M. BOSWARVA and D. B. HOLT, *J. Phys. Chem. Solids* **40** (1979) 567.
35. D. B. HOLT, S. DATTA and I. M. BOSWARVA, *J. Phys. (France)* **41** (1980) C6-522.
36. N. TAKEUCHI, K. INABE and H. NANTO, *Phys. Stat. Sol. (a)* **33** (1976) K125.
37. W. C. LAS and T. G. STOEBE, *J. Mater. Sci.* **16** (1981) 1191.

Received 11 February 1981
and accepted 1 February 1982